Properties and atomic structure of amorphous zirconium

Ristić, Ramir; Babić, Emil

ISSN 1330–0008
CODEN FIZAE4

PROPERTIES AND ATOMIC STRUCTURE OF AMORPHOUS ZIRCONIUM

RAMIR RISTIĆ [a] and EMIL BABIĆ [b]:

[a] *Faculty of Phylosophy, POB 144, HR-31000 Osijek, Croatia*

[b] *Department of Physics, Faculty of Science, POB 331, HR-10002 Zagreb, Croatia*

Paper devoted to honour the memory of Professor Vladimir Šips

Received 11 October 2004; Accepted 21 January 2005
Online 2 December 2005

Wide glass-forming range in Zr-M alloys (M = late transition metal) combined with a simple, often linear, variation of their physical properties with composition makes it possible to deduce physical properties of pure amorphous zirconium. We explore this possibility by using our experimental results for the magnetic susceptibility and superconducting transition temperature of paramagnetic amorphous Zr - (Co,Ni,Cu) alloys extending over a wide composition range. By combining these results with the literature results for the low temperature specific heat of the same alloy systems, we obtained a set of parameters associated with the electronic structure of the amorphous Zr. The comparison of these parameters with the results of the electronic structure calculations for different crystalline phases of Zr and with the results of the atomic structure and initial crystallisation studies of the same alloy systems indicate a fcc-like local atomic structure for amorphous Zr.

PACS number: 75.50. Kj UDC 537.622, 539.213
Keywords: glassy Zr alloys, magnetic susceptibility, structure

1. *Introduction*

Very recently the formation of a bulk metallic glass from the elemental zirconium at high pressure and high temperature has been reported [1]. This is significant achievement since previous attempts to make pure metals amorphous were unsuccessful. Unfortunately, a small size of of the transformed sample allowed only the X-ray diffraction measurements, leaving the physical properties of the amorphous zirconium still unknown. Fortunately, in the case of Zr and probably of other early transition metals (TE), such as Ti and Hf, it seems possible to deduce some physi-

cal properties of a pure amorphous TE from the results for these properties of the amorphous TE-TL alloys (TL are the late transition or noble metals). In particular, for paramagnetic amorphous TE-TL alloys, the properties which are directly related to the electronic density of state (DOS) show simple, often linear variation with TL content over a wide composition range [2 – 7]. These findigs were correlated with Ultraviolet photoemission spectroscopy (UPS) results [8] which showed that over a wide composition range, DOS at the Fermi level (E_F) is dominated by TE d-states. Therefore, the effect of alloying with TL can be approximated with the dilution of amorphous TE [4,5,9].

This idea was recently used by Bakonyi [10] in order to deduce the DOS and local atomic structure of the amorphous Ti, Zr and Hf. In particular, the extrapolation of the literature specific heat (LTSH) and superconductivity data for (Ti,Zr,Hf)-(Ni,Cu) glassy alloys to zero Ni and Cu content was used in order to obtain the bare DOS at E_F ($N_0(E_F)$) for amorphous Ti, Zr and Hf. The obtained $N_0(E_F)$ agreed well with those calculated for cubic (fcc and bcc) crystalline phases of the same metals [11]. On the basis of additional information provided from the atomic structure [12] and crystallisation [13] studies, the author singled out the fcc-like local structure for amorphous Ti, Zr and Hf [10].

Here, we use our magnetic susceptibility and superconductivity results for paramagnetic amorphous Zr-(Co, Ni, Cu) alloys in order to obtain these parameters for amorphous Zr and simultaneously check if these results also support an fcc-like local atomic structure for amorphous Zr. In particular, we extrapolate linearly our measured superconducting transition temperatures as well as the magnetic susceptibilities ($\chi_{\rm exp}$) and their (enhanced) Pauli paramagnetic contributions ($\chi_{\rm p}$) to zero TL content. We also use the literature LTSH data and our superconductivity data to determine the corresponding free-electron value for the Pauli paramagnetism ($\chi^0_{\rm p}$) and calculate the Stoner enhancement factor S. Whereas the extrapolated $\chi_{\rm exp}$ and S agree well with those calculated for crystalline fcc Zr [11] the derived values for $\chi_{\rm p}$ and $\chi^0_{\rm p}$ agree better with the calculation for an bcc structure [11]. The possible origin for this ambiguity is briefly discussed.

2. Experimental procedures

The amorphous $Zr_{100-x}Cu_x$ ($26 \leq x \leq 71$), $Zr_{100-x}Ni_x$ ($22 \leq x \leq 67$) and $Zr_{100-x}Co_x$ ($19 \leq x \leq 35$) alloys were prepared by the melt-spinning of master alloys with the predetermined concentration [14]. The resulting ribbons were about 2 mm wide and 20 – 30 μm thick. The static magnetic susceptibility $\chi_{\rm exp}$ was measured on samples weighting few miligrams with the Faraday method [5]. The absolute values of $\chi_{\rm exp}$ were accurate to about one percent, while the relative accuracy was about 0.1%. Our $\chi_{\rm exp}$ data [5] agree very well with later results for the same alloy systems [15]. Since $\chi_{\rm exp}$ for all our alloys showed very weak temperature dependence ($< 10^{-5}$ JT^{-2}mol^{-1} from 4.2K to 273K), we used the values of $\chi_{\rm exp}$(273 K) in our analysis.

The superconducting transition temperatures T_c were obtained either resistively

by using an AC four-probe method on approximately 3 cm long samples [16] or from the AC susceptibility measurements [14]. Our values for T_c agree very well with other published results [10,15,17] for the same alloy systems. Some data relevant to our Zr-Co alloys are given in Table 1, whereas those for Zr-Cu and Zr-Ni alloys were previously published [18]. The extracted parameters for amorphous zirconium are listed in Table 2.

TABLE 1. Data relevant to Zr-Co *amorphous alloys: T_c is the superconducting transition temperature, $\chi_{\rm exp}$ is the measured magnetic susceptibility at 273* K, $\chi_{\rm p} = \chi_{\rm exp} - \chi_{\rm ion} - \chi_{\rm orb}$, $\chi^0_{\rm p}$ *is the Pauli susceptibility calculated from $N_0(E_F)$ and S is the Stoner factor.*

$Zr_{100-x}Co_x$	T_c (K)	$\chi_{\rm exp} \times 10^3$ ($JT^{-2}mol^{-1}$)	$\chi_{\rm p} \times 10^3$ ($JT^{-2}mol^{-1}$)	$\chi^0_{\rm p} \times 10^3$ ($JT^{-2}mol^{-1}$)	S
$Zr_{81}Co_{19}$	3.9	1.54	0.86	0.50	1.72
$Zr_{78}Co_{22}$	4.3	1.53	0.84	0.49	1.71
$Zr_{75}Co_{25}$	3.63	1.55	0.85	0.48	1.77
$Zr_{67}Co_{33}$	2.8	1.55	0.84	0.46	1.84
$Zr_{65}Co_{35}$	2.7	1.57	0.86	0.45	1.90

TABLE 2. The extracted parameters of amorphous zirconium compared with those calculated for different crystalline phases of Zr *[11].*

	$N_0(E_F)$ $\left(\frac{\text{states}}{\text{eV atom}}\right)$	$\chi^0_{\rm p} \times 10^3$ ($JT^{-2}mol^{-1}$)	$\chi^0_{\rm p} \times 10^3$ ($JT^{-2}mol^{-1}$)	S	$\chi^0_{\rm p} \times 10^3$ ($JT^{-2}mol^{-1}$)	T_c (K)
α(hpc)	0.96	0.31	0.42	1.35	1.08	0.8
β(bcc)	1.55	0.50	0.88	1.75	1.7	5.8
fcc (a = 0.44 nm)	1.34	0.43	0.69	1.60	≈1.50	
extrapolated values	1.55	0.52	0.84	1.60	1.52	5.7

3. Results

The magnetic susceptibilities ($\chi_{\rm exp}$) of all Zr-M glassy alloys [5,15] are sizably higher than those expected for paramagnetic intertransition metal alloys, and even for the Cu content 26 at% (Fig. 1), $\chi_{\rm exp}$ is higher than that of crystalline (hcp) Zr [5,11]. This finding is consistent with the results of UPS [8] which show that $N_0(E_F)$ is higher in Zr based glasses than in crystalline (hcp) Zr. In amorphous

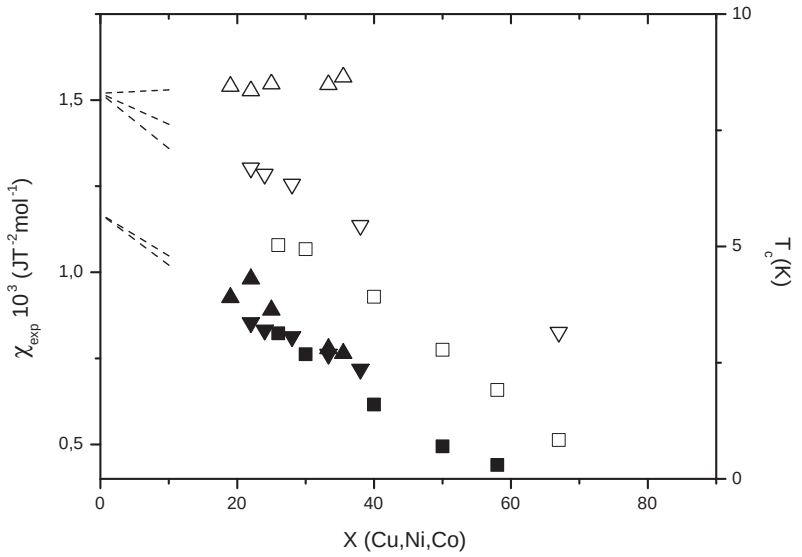

Fig. 1. Measured magnetic susceptibility $\chi_{\rm exp}$ *of amorphous* $Zr_{100-x}Co_x$ ($\triangle$), $Zr_{100-x}Ni_x$ ($\triangledown$), $Zr_{100-x}Cu_x$ ($\square$) *alloys versus* x *(left scale). The same symbols but full show the variation of superconducting transition temperatures* T_c *with* x *for the same alloys (right scale). Dashed lines extrapolate the data to* $x = 0$.

alloys containing Cu and Ni, $\chi_{\rm exp}$ decreases approximately linearly with the Cu and Ni content, whereas in Co containing glasses, it remains constant within the explored concentration range (Fig. 1, Table 1). However, for all three alloy systems, the extrapolation of $\chi_{\rm exp}$ results in Fig. 1 to zero M content yields $\chi_{\rm exp} \approx 1.52\ 10^{-3}$ $\mathrm{JT^{-2}mol^{-1}}$ for amorphous Zr, which agrees very well with the estimate based on DOS calculation for fcc Zr, $\chi_{\rm exp} \approx 1.5\ 10^{-3}$ $\mathrm{JT^{-2}mol^{-1}}$ [11]. Simultaneously, T_c decreases aproximately linearly with increasing M content (Fig. 1) for all three alloys [5,10,15], which shows that the superconductivity in these alloys is determined primarily by the Zr d-electrons. The extrapolation of T_c data to zero M content yields $T_c = 5.7 \pm 0.1$ K for amorphous Zr which agrees well with the finding for bcc Zr, $T_c \simeq 5.8$ K [11]. We note that published data for T_cs of other paramagnetic amorphous Zr-M alloys, such as Zr-Fe [15] and Zr-Pd,Rh [17], also yield practically the same T_c for amorphous Zr. Therefore, our estimate of T_c for amorphous Zr is quite reliable. In order to proceed with the analysis, we have to single out the contributions to measured magnetic susceptibility.

$\chi_{\rm exp}$ of the nonmagnetic transition metal is given as

$$\chi_{\rm exp} = \chi_{\rm p} + \chi_{\rm ion} + \chi_{\rm orb}\,, \tag{1}$$

where $\chi_{\rm ion}$ and $\chi_{\rm orb}$ are the ionic-core diamagnetism and the orbital magnetism with the Landau contribution included, respectively. The Pauli paramagnetism of

the d-band $\chi_{\rm p}$ is enhanced over the free-electron value $\chi_{\rm p}^0 = 2\mu_B^2 N_0(E_F)$ due to the Stoner exchange interaction; $\chi_{\rm p} = S\chi_{\rm p}^0$, where $S = (1 - I_{\rm eff} N_0(E_F))^{-1}$ is the Stoner enhancement factor and $I_{\rm eff}$ is the effective exchange integral within the d-band.

In order to obtain $\chi_{\rm p}$ for each alloy, we subtracted from $\chi_{\rm exp}$ the corresponding contributions $\chi_{\rm ion}$ and $\chi_{\rm orb}$ derived from the results of Ref. [18]. In particular, we scaled the values of $\chi_{\rm ion}$ [19] and $\chi_{\rm orb}$ [11,20] of particular element to their atomic fraction in a given alloy. Since the values of $\chi_{\rm ion}$ are quite small, the uncertainty in these values cannot affect the results of our analysis. However, $\chi_{\rm orb}$ of Zr is large [11] and strong decrease of $\chi_{\rm exp}$ with x for Zr-Cu and Zr-Ni alloys (Fig. 1) is mainly due to decrease of the overall $\chi_{\rm orb}$ with x [9,18]. Therefore, the uncertainty in the value of $\chi_{\rm orb}$ for Zr may affect our results for $\chi_{\rm p}$. However, $\chi_{\rm orb}$ is farly insensitive to the crystal structure [11] and hence we do not expect any large effects associated with the uncertainty in the actual value of $\chi_{\rm orb}$ taken for Zr. The resulting data for $\chi_{\rm p}$ of all our alloys are shown in Fig. 2.

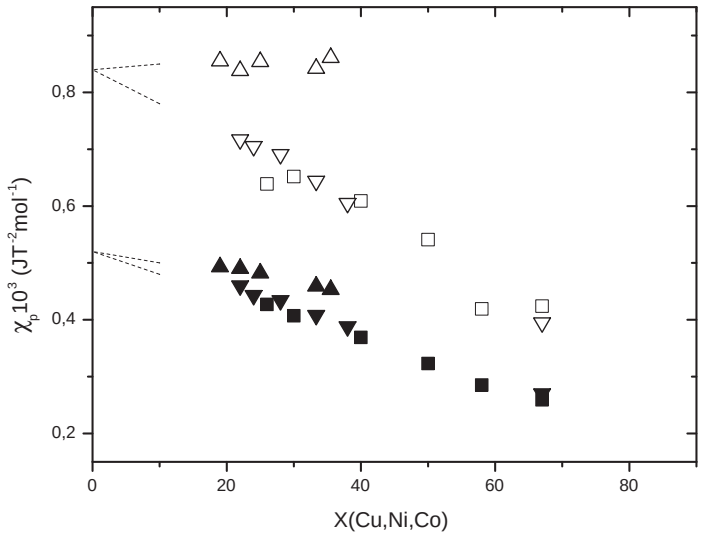

Fig. 2. $\chi_{\rm p}$ *of* $Zr_{100-x}Co_x$ ($\triangle$), $Zr_{100-x}Ni_x$ ($\triangledown$), $Zr_{100-x}Cu_x$ ($\square$) *alloys versus* x. *The same symbols but full represent dependence of* $\chi_{\rm p}^0$ *versus* x *for the same alloys. Dashed lines extrapolate the data to* $x = 0$.

Like $\chi_{\rm exp}$, $\chi_{\rm p}$ also shows a linear variation with x for all three alloy systems. These variations extrapolate to $\chi_{\rm p} \simeq 0.84\ 10^{-3}$ JT^{-2}mol^{-1} for $x = 0$ (Fig. 2.). This value of $\chi_{\rm p}$ for amorphous Zr agrees well with that calculated for bcc Zr ($0.88\ 10^{-3}$ JT^{-2}mol^{-1} [11]). As expected from the "dilution effects" [8,9], the variations of $\chi_{\rm p}$ with x for M = Cu and Ni are essentially the same. For these two alloy systems, the variations of $N_0(E_F)$ vs. x were also practically the same [10]. Therefore, we expect the same $\chi_{\rm p}^0$ vs. x variations and hence the same Stoner enhancement factor S for these alloy systems. However, in Zr-Co alloys, $\chi_{\rm p}$ is nearly constant (Table 1,

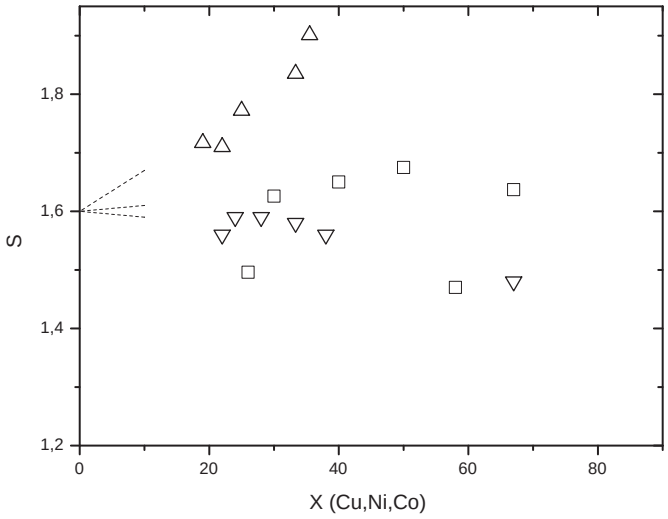

Fig. 3. The Stoner factor of $Zr_{100-x}Co_x$ (△), $Zr_{100-x}Ni_x$ (▽), $Zr_{100-x}Cu_x$ (□) *alloys versus* x. *Dashed lines extrapolate the data to* $x = 0$.

Fig. 3) which means that in this system $N_0(E_F)$ and/or S are enhanced with respect to the corresponding quantities of Zr-Cu and Zr-Ni alloys. In order to resolve this problem, we combined our data for T_c with the corresponding literature LTSH data [6,7,21] and derived $N_0(E_F)$ for all our alloys. From $N_0(E_F)$ data (Table 1 and Refs. [10] and [18]), we calculated the corresponding $\chi_{\rm p}^0$ values which are also shown in Fig. 2. The $\chi_{\rm p}^0$ vs. x (hence also $N_0(E_F)$ vs. x) variations for the three alloy systems are very similar and consistent with the dilution effects. All three variations extrapolate (Fig. 2) to $\chi_{\rm p}^0 = 0.52\ 10^{-3}$ JT^{-2}mol^{-1} for $x = 0$, which corresponds to $N_0(E_F) = 1.55$ states/(eV atom). The extracted values for $\chi_{\rm p}^0$ and $N_0(E_F)$ of amorphous Zr agree very well with those calculated for bcc Zr [11] and are again some 15% higher than those for hypotetic fcc Zr [11]. Simultaneously, our $\chi_{\rm p}^0$ and $N_0(E_F)$ are almost two times larger than those observed for hcp Zr, which rules out hcp-like local structure for amorphous Zr. As seen from the variations of $\chi_{\rm p}^0$ with x, the enhancement of $\chi_{\rm p}$ values of Zr-Co alloys with respect to those for Zr-Cu and Zr-Ni alloys are mainly due to progressive enhancement of the Stoner enhancement factor $S = \chi_{\rm p}/\chi_{\rm p}^0$ with x in Zr-Co alloys.

Figure 3 shows that S is approximately constant for Zr-Cu and Zr-Ni alloys, whereas it increases aproximately linearly with Co content in Zr-Co alloys. This enhancement of S with x in our Zr-Co alloys is consistent with the onset of ferromagnetism observed at elevated x in these alloys [15]. Moreover, our results for S of Zr-Co alloys are consistent with the $I_{\rm eff}$ and $N_0(E_F)$ values for similar alloys in Ref. [15]. Relatively large scatter of the data for S at large x is due to the sensitivity of S to $I_{\rm eff}N_0(E_F)$; a small change in either $I_{\rm eff}$ or $N_0(E_F)$ produces sizeable change in S. This is probably the reason why most authors prefer to present their

results in terms of I_{eff} rather than S. In spite of that, our data for S allow a quite accurate extrapolation to $x = 0$. We obtain (see Fig. 3) $S = 1.6$ for amorphous Zr which agrees very well with that calculated for fcc Zr (1.6), it is about 10% lower than that for bcc structure [11] and is well above that for hcp Zr. We note that the enhancement of S in amorphous Zr with respect to that in crystalline (hcp) Zr is mainly due to the enhancement of $N_0(E_F)$ [9]. In particular, the value of I_{eff} of amorphous Zr is nearly the same as that of hcp Zr [9,11].

4. Discussion

In Table 2, we compare the extracted parameters of amorphous Zr with those for different crystalline phases of Zr [11]. Our results for χ_{exp}, T_c, χ_{p}^0 and S of amorphous Zr obtained by linear extrapolation of the results for paramagnetic amorphous Zr-M alloys agree quite well with experimental (bcc) and calculated results for cubic phases (bcc and fcc) of a pure crystalline Zr [11]. Simultaneously, all our results for amorphous Zr are considerably larger than those for stable crystalline hcp phase of Zr. This is plausible since the amorphous atomic structure is incompatible with the high anisotropy of the hcp lattice. Since our results for χ_{exp} and S agree rather better with the calculations for the fcc Zr, whereas those for T_c and χ_{p}^0 (hence also $N_0(E_F)$) are consistent with the experimental and calculated results for bcc Zr [11], these results alone cannot tell us whether a fcc-like or bcc-like structure adequately represents the local atomic structure of amorphous Zr. However, the coordination numbers in Zr-M amorphous alloys $Z \approx 12$ are close to those of a fcc-like local structure [12] and the metastable phases appearing first upon the crystallisation of these alloys also have the fcc structure [13]. Therefore, the bcc-like local structure of amorphous Zr is quite unlikely and the question arises what makes the interpretation of our results in terms of the results calculated in Ref. [11] ambiguous?

The uncertainties in our and literature experimental results (Figs. 1 and 2) are small and cannot amount to the required $\pm 10\,\%$ percent difference. Our extrapolation procedure is also quite reliable: the data extend over a wide composition range and in the case of χ_{exp} and χ_{p}, the extrapolated values have the constant values obtained for Zr-Co alloys. Moreover, even the nonlinear extrapolation (such as the saturation) of our (Fig. 2) and literature data [10] for $x < 19$ cannot account for the 15 percent difference between the values calculated for the two cubic structures of Zr [11].

Therefore, the root of the problem is probably the uncertainty inherent to the band structure calculations (estimated to about $10\,\%$ in the case of Zr [11]). In particular, the assumed lattice parameter $a = 0.44$ nm [11] for fcc Zr is, as expected, somewhat smaller than that obtained from the extrapolation of k_p (modulus of the scattering vector corresponding to the position of the first maximum of the diffraction pattern) values (Fig.4) for amorphous Zr-(Co,Ni,Cu) to $x = 0$ [22,23]. From k_p, we can obtain an approximate value for the mean interatomic distance [24]

$$d = \frac{7.73}{k_p}\,. \tag{2}$$

If we extrapolate k_p in Fig. 4 to $x = 0$, we get $k_p = 2.33$, from (2) $d = 3.31\ 10^{-10}$, and for fcc structure $a = 0.46$ nm. We believe that the resulting difference in the unit cell volumes for the amorphous and that assumed for fcc crystalline Zr [11] may be sufficient in order to explain the observed differences between the experimental results for amorphous Zr and those calculated for the crystalline fcc Zr. Indeed, as pointed out by Bakonyi [25], if one takes the unit cell volume for amorphous Zr the same as that for hcp Zr (which is larger than that for bcc Zr), one obtains $N_0(E_F) \approx 1.55/(\text{ atom eV})$ which is the same as that calculated for bcc Zr (Table 2).

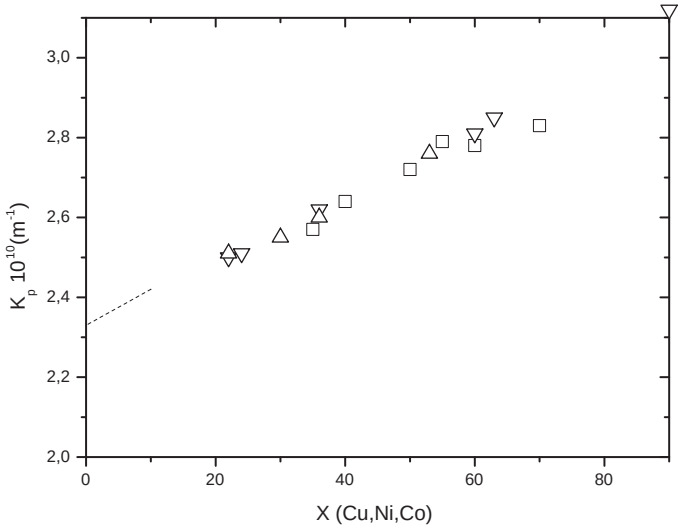

Fig. 4. Modulus of the scattering vector corresponding to the position of the first maximum of the diffraction pattern k_p of $Zr_{100-x}Co_x$ (△), $Zr_{100-x}Ni_x$ (▽), $Zr_{100-x}Cu_x$ (□) alloys versus x [22,23]. Dashed line extrapolates the data to $x = 0$.

5. Conclusion

Linear variations of the superconducting transition temperature T_c, the magnetic susceptibility χ_{exp} (and its components χ_{p} and χ^0_{p}) and the bare density of states at E_F, $N_0(E_F)$ [10], in paramagnetic amorphous $Zr_{100-x}M_x$ alloys (M=Co, Ni and Cu; $x \leq 70$) are used in order to obtain the parameters for amorphous Zr. The extrapolations of these variations to $x = 0$ (pure Zr) yields for all three systems the same parameters: $T_c = 5.7$ K, $\chi_{\text{p}} = 0.84\ 10^{-3}$ $\text{JT}^{-2}\text{mol}^{-1}$, $\chi^0_{\text{p}} = 0.52\ 10^{-3}$ $\text{JT}^{-2}\text{mol}^{-1}$ and $S = 1.6$. The comparison of these parameters with the results of the band structure calculation for different crystalline phases of Zr [11] suggests an approximately cubic (fcc or bcc) local atomic structure in amorphous Zr. This ambiguity (fcc or bcc like) is probably due to too small unit cell volume assumed for fcc Zr in Ref. [11], as evidenced from the information gained from the atomic

structure studies of the investigated alloy systems [22,23].

Indeed, the assumption [25] that the unit cell of the fcc Zr phase is the same as that of the hcp one leads to the $N_0(E_F)$ value which is the same as our (extrapolated) $N_0(E_F)$ for amorphous Zr. This in turn makes the parameters in Table 2 consistent with a fcc-like local atomic structure of amorphous Zr. Further evidence for the fcc-like atomic structure is provided by the initial crystallisaton studies of amorphous Zr-Fe, Co, Ni alloys [13]. In all these alloy systems, the crystallisation started with the metastable phases showing a fcc symetry. However, recent neutron diffraction studies of undercooled liquid Zr indicate an icosahedral short-range atomic structure [26]. Therefore, the actual local atomic structure of amorphous Zr may still be uncertain.

Finally, we note that the magnetic (paramagnetic) parameters derived in this work do not exaust the list of the properties of amorphous Zr which can be extracted from the results of systematic studies of amorphous Zr-M alloy systems [3,4,5,9,10]. This work is now in progress.

Acknowledgements

We thank Dr. Marko Miljak for the help with the magnetic susceptibility measurements and Dr. Imre Bakonyi for useful discussions.

References

[1] Jianzhong Zhang and Yusheng Zhao, Nature **430** (2004) 332.

[2] H. Beck and H.-J. Gntherodt, eds., *Glassy Metals III*, Topics in Applied Physics, Vol. 72, Springer, Berlin (1994), and reference therein.

[3] J. Ivkov and E. Babić, J. Phys. Cond. Matter. **2** (1990) 3891, and reference therein.

[4] Ž. Marohnić, E. Babić, M. Guberović and G. J. Morgan, J. Non-Cryst. Solids **105** (1988) 303.

[5] E. Babić, R. Ristić, M. Miljak, M. G. Scott and G. Gregan, Solid State Commun. **39** (1981) 139; E. Babić, R. Ristić, M. Miljak and M. G. Scott in *Proc. 4th Int. Conf. On Rapidly Quenched Metals*, eds. T.Masumoto and K. Suzuku, Sendai, Japan (1982) 1079.

[6] G. von Minigerode and K. Samwer, Physica B+C **107** (1981) 1217.

[7] M. Matsuura and U. Mizutani, J. Phys. F: Metal Phys. **16** (1986) L183.

[8] P. Oelhafen, E. Hauser and H.-J. Güntherodt, Solid State Commun. **35** (1979) 1017.

[9] R. Ristić, E. Babić, K. Šaub and M. Miljak, Fizika (Zagreb) **15** (1983) 363.

[10] I. Bakonyi, J. Non.-Cryst. Solids **180** (1995) 131, and reference therein.

[11] I. Bakonyi, H. Ebert and A. I. Liechenstein, Phys. Rev. B **48** (1993) 7841.

[12] W.-M. Kuschke, P. Lamparter and S. Steeb, Z. Naturforsch. **46a** (1991) 951; F. Paul and R. Frahm, Phys. Rev. B **42** (1990) 10945; X. L. Yeh and E. J. Cotts, J. J. Mater. Res. **2** (1987) 173.

[13] S. Brauer, J. O. Strom-Olsen, M. Sutton, Y. S. Yang, A. Zaluska, G. B. Stephenson and U. Köster, Phys. Rev. B **45** (1992) 7704.

[14] E. Babić, S. Butcher, R. K. Day and J. B. Dunlop, *Proc. 5th Int. Conf. On Rapidly Quenched Metals*, eds. S. Steeb and H. Warlimont, Elsevier, Amsterdam (1985) 1157.

[15] Z. Altounian and J. O. Strom-Olsen, Phys. Rev. B **27** (1983) 4149; E. Batalla, Z. Altounian and J. O. Strom-Olsen, Phys. Rev. B **31** (1985) 577.

[16] R. Ristić, Ž. Marohnić and E. Babić, Mater. Sci. Eng. A **226-228** (1997) 1060.

[17] M. G. Karkut and R. R. Hake, Phys. Rev. B **28** (1983) 1396.

[18] R. Ristić, Ž. Marohnić and E. Babić, Fizika A (Zagreb) **12** (2003) 89, and reference therein.

[19] J. Banhart, H. Ebert and J. Voitlnder, J. Magn. Magn. Mater. **61** (1986) 221.

[20] C. M. Place and P. Rhodes, phys. stat. sol. (b) **47** (1971) 475.

[21] S. Kanemaki, O. Takehira, K. Fukamichi and U. Mizutani, J. Phys.: Condens. Mater. **1** (1989) 5903.

[22] Y. Calvayrac, J. P. Chevalier, M. Harmelin, A. Quivy and J. Bigot, Phil. Mag. B **48** (1983) 323.

[23] K. H. J. Buschow and N. M. Beekmans, Phys. Rev. B **19** (1979) 3843.

[24] A.Guinier, *X-ray Diffraction*, Dover Publications, New York (1994).

[25] I. Bakonyi, private communication (2004).

[26] T. Schenk, D. Holland Moritz, V. Simonet, R. Bellisent and D. M. Herlach, Phys. Rev. Lett. **89** (2002) 75507.

SVOJSTVA I ATOMSKA STRUKTURA AMORFNOG CIRKONIJA

Široko područje koncentracija za dobivanje staklastih Zr-M slitina (M = kasni prijelazni metal) u svezi s jednostavnim, često linearnim, promjenama fizičkih svojstava sa sastavom omogućuje određivanje fizičkih svojstava čistog amorfnog cirkonija. To smo istraživali rabeći naše eksperimentalne rezultate za magnetsku susceptibilnost i temperature supravodljivog prijelaza za paramagnetske amorfne Zr-(Co,Ni,Cu) slitine u širokom području koncentracija. Povezujući te rezultate s podacima iz literature za specifični toplinski kapacitet na niskim temperaturama za te slitine, dobili smo skup parametara pridruženih elektronskoj strukturi amorfnog cirkonija. Usporedba tih parametara s rezultatima računa elektronske strukture za različite kristalne faze Zr, te rezultatima studija atomske strukture i početne kristalizacije tih slitina, ukazuje na atomsku strukturu sličnu fcc za amorfni Zr.